

Interference Analysis of an Heavy Lift Multirotor Drone Flow Field and Transported Spraying System

Fabrizio Sarghini*, Angela De Vivo

University of Naples Federico II, Department of Agricultural Sciences, Naples, Italy
fabrizio.sarghini@unina.it

Drones in agriculture can be used for a variety of different task, aimed to increase farm crop yields and/or accurately monitor growth status, simultaneously decreasing time, labour and resources. While for some specific task a medium size drone can be used, on the other hand for more intensive task like for example precision spraying of pesticide or fertilizer, an heavy lift drone is more appropriate.

A growing momentum application consists in the possibility to use heavy lift drones for precision pesticide distribution.

A report by the Association for Unmanned Vehicle Systems International (AUVSI) found that so-called "precision agriculture" will make up about 80% of the United States UAS market.

Some of the multirotor already on the market are designed to spray large areas of farmland with pesticides or fertilizers, covering an extraordinary amount of distance quickly – 4,000-6,000 m² in just 10 minutes and reducing the amount of pesticide from 20% to 40%, with no exposure to risk for human being.

The optimal design of transported spraying equipment requires a careful study of fluid dynamics interactions of the downwash wakes generated from the rotors and the spraying nozzle of horizontal or vertical bars.

Experimental setups finalised to drones spraying analysis are complex to use, and the final results are strongly influenced by the operative and environmental conditions.

A powerful tool for a preliminary investigation of such interactions is provided by computational fluid dynamics, allowing a predictive analysis of possible wash down wake effects with spraying operative setup.

And in this work a CFD analysis of two different configurations (X6 and Y6 multirotors) is presented.

The knowledge of aerodynamic effects will allow the optimisation of boom position and a correct setup of the discharge rate of chemical liquid according to the flying speed of the UAV..

1. Introduction

Although many national regulations still lack of full comprehension of the benefit that the use of drones can introduce in several economic activities, their use in precision agriculture seems to gain momentum year by year (Zhang et al. 2012).

They can be used in several activities, like for example in soil and field investigations to produce precise 3-D maps for early soil analysis, useful in planning seed planting patterns. Moreover, after planting, drone-driven soil analysis provide data for irrigation and nitrogen-level management. Planting activities can be performed using UAV as well: drone-planting systems that achieve an uptake rate of 75 percent and decrease planting costs by 85 percent are already present on the market. More advanced systems can shoot pods with seeds and plant nutrients into the soil, providing the plant all the nutrients necessary to sustain life (MIT Technology Review,2015).

Crop spraying is an emerging activity that can be provided by UAVs: the use of distance-measuring equipment—like ultrasonic echoing and lasers such as those used in the light-detection and ranging, or LiDAR, method—enables a drone to adjust flying altitude as the topography and geography varies, avoiding collisions. As a consequence drones can scan the ground and spray the correct amount of liquid, modulating the distance from the ground and spraying in real time pesticides or fertilizer for even coverage. (Anthony et al., 2012)

The result: increased efficiency with a reduction of in the amount of chemicals penetrating into groundwater, and experts estimate that aerial spraying can be completed up to five times faster with drones than with traditional machinery. Another important activity that could be performed by drones is crop monitoring: vast fields and low efficiency in crop monitoring coupled together create one of the major farming's obstacle. Such monitoring activities are exacerbated by unpredictable weather conditions, increasing risk and field maintenance costs. (Colomina et al. ,2014) Satellite imagery offered the most advanced form of monitoring, but drawbacks are still present: images had to be ordered in advance, and they could be taken only once a day at the best, with a resolution not comparable with UAV imaging systems. Moreover, services were extremely costly and the images' quality typically suffered on certain days depending on the clouds. On the contrary time-series animations taken by UAV can show the precise development of a crop and reveal production inefficiencies, enabling better crop management. The use of hyperspectral, multispectral, or thermal sensors can identify which parts of a field require water, and once the crop is growing, drones allow the calculation of the vegetation index, which describes the relative density and health of the crop, and show the heat signature, the amount of energy or heat the crop emits (Primicerio et al. 2012, Hassan-Esfahani et al. 2014). Crop monitoring is essential to assess crop health and spot bacterial or fungal infections on trees as well. By scanning a crop using both visible and near-infrared light, drone-carried devices can identify which plants reflect different amounts of green light and NIR light. Such information can produce multispectral images which are to track changes in plants, to assess their health. (Costa et al, 2012), and to provide a fast response to infestations that can save an entire orchard. In addition, as soon as a problem is discovered, farmers can apply and monitor remedies more precisely, increasing plant's ability to overcome the incoming disease.

Regulations in Italy allow the possible use of drones inside the limit of 25 kg as maximum take-off weight without significant difficulties, while heavier UAVs require a certification level similar to civil airplanes. In such class of vehicles (max 25 kg), several possible degrees of freedom in terms of power and configurations are introduced, depending on the service required.

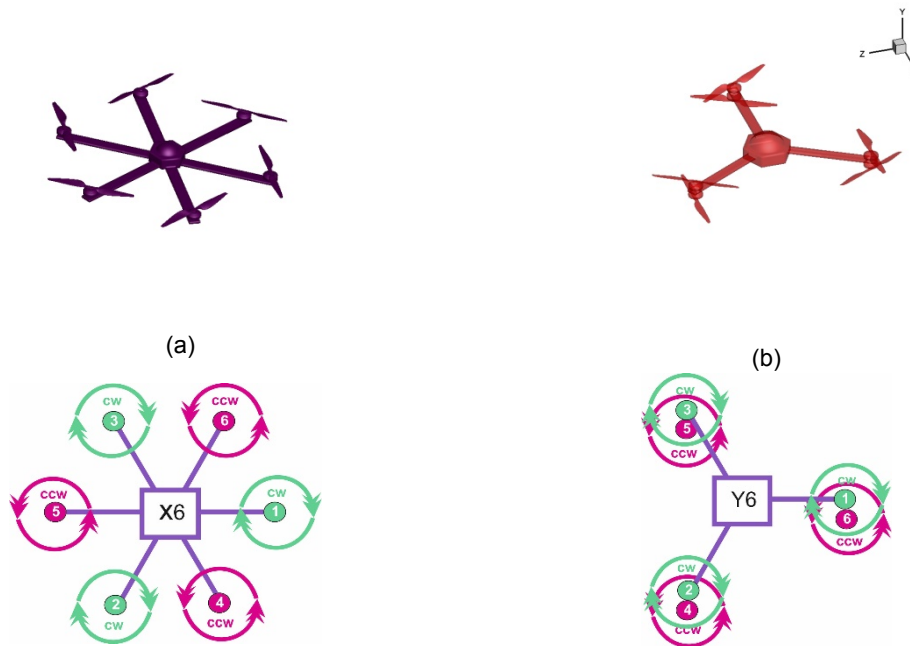


Figure 1. Multirotor X6 (a) and Y6 (b) configurations

In this work two different configurations, showed in Figure 1a and Figure 1b were analysed: an hexacopter with 6 motors mounted on 6 arms (X6) 60° apart on a symmetric frame, with three sets of CW and CCW propellers, and a Y6 coaxial configurations with 6 motors mounted on 3 arms 120° apart.

X6 configuration is similar to the quadcopter, but it provides more lifting capacity due to the larger number of motors. It's also possible that in case one motor fails, the aircraft can still land safely. The downside is that they tend to be larger in size and more expensive. The Y6 has 6 motors arranged in a "Y" shape frame, which similar in shape to a tricopter but with two motors per arm, one above and one below. Also in this case the

drone presents 6 motors in total. It uses both CW and CCW propellers on the same arm, rather than a servo to enable yaw. In this way the comparison can be done with the same nominal lift power. This type of multicopter can be made more compact (as big as a tricopter) for the similar lifting capability as the hexacopter. However it is less efficient due to the coaxial motor-arrangement.

In Y6 or Y8 multicopter configurations, a coaxial motor-arrangement is present. Such configuration introduces some pros and cons. A major advantage of a coaxial motor-arrangement is linked to the fact that if one motor fails you can still land safely, and moreover it saves space and it is easier to make the frame foldable to carry around.

Among the disadvantages, we can notice that bottom propellers can get caught easily as pilots can't oversee them so simply. The propellers are on both top and bottom levels of the arms, so they will easily appear on the camera view, although it is possible to place the camera in the middle of the aircraft – between the motors, trying to minimize such interference.

If we consider the aerodynamics, in coaxial configurations it is possible to notice a 10-20% loss in power/efficiency respect to the in-plane configuration, because basically the bottom motor is just moving in already accelerated downwash. It is possible to minimize such losses by using longer/higher pitch propellers or a higher rpm motor.

Last but not least, it is more difficult to find an appropriate landing gear because it can't be mounted that far out on the arm.

The motor configurations considered in this work are based on T.Motor U Type U11 motors, KV=120 running at 65% of efficiency at 2535 rpm, with an overall nominal thrust of almost 25 kg, near the maximum take off weight limit allowed for this class of UAV. A 28"x9.2 carbon fibre propeller (3 set including CW & CCW blades) was adopted. An hovering configuration was analysed in this work. Temperature was set to 26°C.

2. Materials and Methods

2.1 Numerical method

A moving mesh approach was used to model propeller dynamics, using Openfoam 2.2 CFD numerical code, inside a compressible flow framework. The continuity equation (1), momentum equation (2) and energy equation (3) for a compressible fluid can be written as follows

$$\frac{\partial \rho}{\partial t} + \frac{\partial}{\partial x_j} [\rho u_j] = 0 \quad (1)$$

$$\frac{\partial}{\partial t} (\rho u_i) + \frac{\partial}{\partial x_j} [\rho u_i u_j + p \delta_{ij} - \tau_{ji}] = 0, \quad i = 1,2,3 \quad (2)$$

$$\frac{\partial}{\partial t} (\rho e_o) + \frac{\partial}{\partial x_j} [\rho u_j e_o + u_j p + q_j - u_i \tau_{ij}] = 0 \quad (3)$$

For a Newtonian fluid, assuming that Stokes law is valid, the viscous stress is given by:

$$\tau_{ij} = 2\mu S_{ij}^* \quad (4)$$

Where the trace-less viscous strain-rate is defined by:

$$S_{ij}^* \equiv \frac{1}{2} \left(\frac{\partial u_i}{\partial x_j} + \frac{\partial u_j}{\partial x_i} \right) - \frac{1}{3} \frac{\partial u_k}{\partial x_k} \delta_{ij} \quad (5)$$

The heat-flux, q_j , is given by Fourier's law as:

$$q_j = -\lambda \frac{\partial T}{\partial x_j} \equiv -C_p \frac{\mu}{Pr} \frac{\partial T}{\partial x_j} \quad (6)$$

Where the laminar Prandtl number, Pr is defined by:

$$Pr \equiv \frac{c_p \mu}{\lambda} \quad (7)$$

The total energy, e_o , is defined by:

$$e_o \equiv e + \frac{u_k u_k}{2}$$

Bounded second order central differences were adopted for convective terms, and a second order scheme was adopted for advancement in time.

The presence of turbulence was included by adopting a Large Eddy simulation approach. A 3×10^6 CV grid was adopted, but given the complexity of the flow field such grid is probably under-resolved, and results should be considered to provide a qualitative point of view.

3. Results and Discussion

Downwash effects can be computed both in terms of wake intensity and homogeneity of perturbed field.

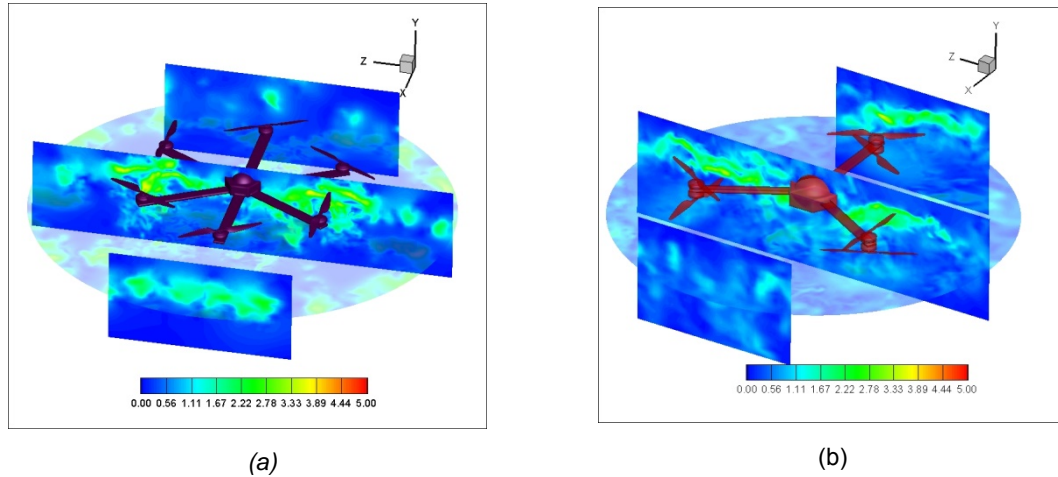


Figure 2. . Instantaneous snapshot of velocity magnitude on a vertical planes for X6(a) and Y6(b) configurations.

Positioning a spray system in the most perturbed part of the flow field would result in an increased probability of off-target pesticide distribution, and the risk is present also in the case in which a granular product is adopted to bypass regulations' restrictions.

Figure 2 shows the velocity magnitude contours in 3 vertical planes, showing in both cases local peaks of velocity appearing on the plane near the propellers as expected.

In Figure 3 the instantaneous velocity magnitude flow field is reported on an horizontal plane, showing in the case of Y6 configuration a more uniform velocity distribution with local peaks of minor intensity respect to the X6 configuration, but with a more extended interference area.

On the other hand, a possible collocation of spraying or granular distribution systems in the dead zones of X6 configuration (requiring an appropriate balancing of the payload) could minimize dispersion effects.

If the payload is collocated in central position, x6 configuration seems to provide a better shield than Y6 configuration. Moreover, further shielding could be provided by auxiliary systems not directly interfering with propellers downwash.

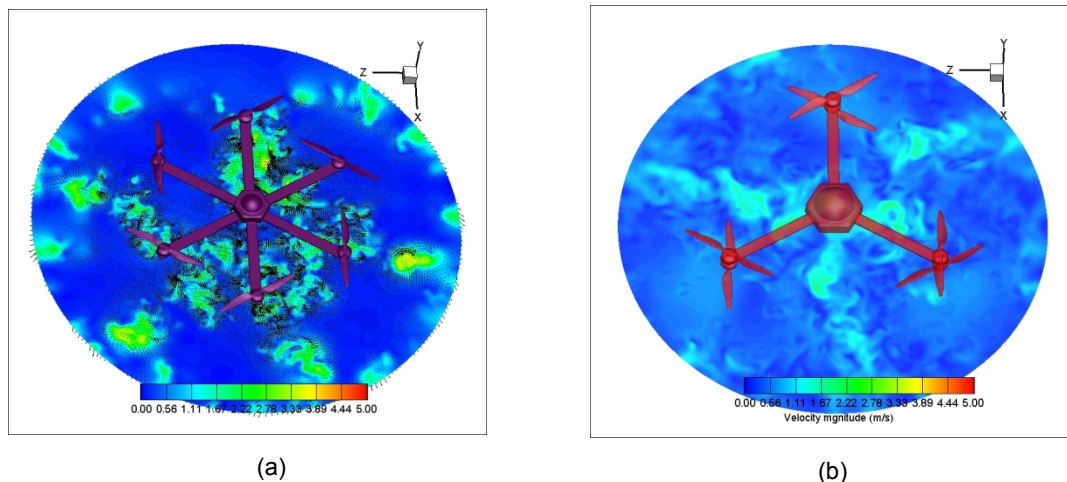


Figure 3. Instantaneous snapshot of velocity magnitude on a transversal plane 0.28m under the propellers midplane .

In Figure 4, vorticity magnitude is shown, highlighting also in this case a minor intensity for the Y6 case.

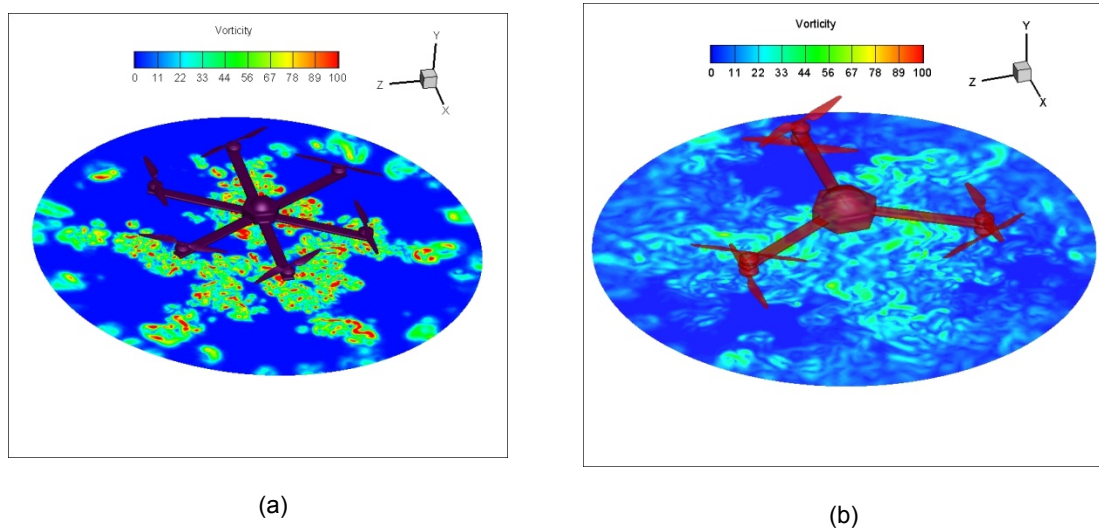


Figure 4. Variation of vorticity magnitude for X6 (a) and Y6 (b) configuration.

In Figure 4 vorticity distribution in both configurations is presented, and also in this case more intense but more localized peaks are present in X6 configuration.

In Figure 5 an instantaneous snapshot of droplet distribution is shown for an advancement speed of the UAV equal to 5 m/s. The counter-rotating flow field seems to introduce an entrapment effect on a substantial part of the drops into the propeller wake, with possible droplet-droplet interactions and a deposition delay respect to the hypothetical target.

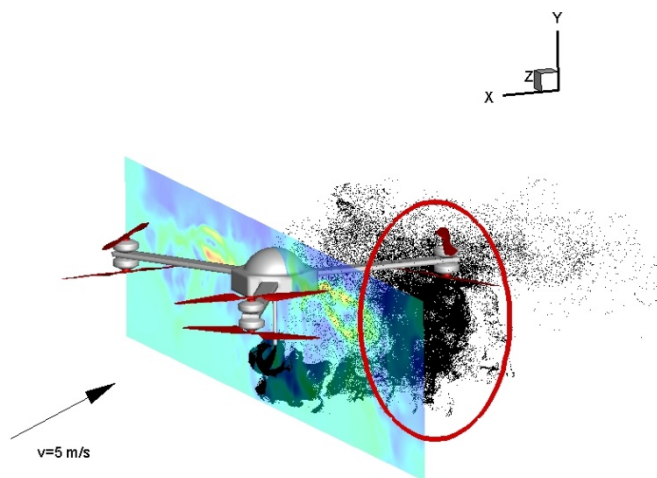


Figure 5. Entrapment effect on droplets into propellers' wake

4. Conclusions

Different design choices seem to have a consistent impact on the flow field embedding the drone, and CFD is a powerful tool to provide indications about possible collocation of auxiliary spraying or granular distribution systems.

The Y6 configuration seems to generate an increased downwash effect in terms of extension but with reduced intensity, probably due to the interactions of counter-rotating pairs of propellers. On the other hand, in such

configuration a consistent disturbance is generated on three main directions 120° apart from the main axis of symmetry. An important entrainment phenomena into propellers' wake is present in Y6 configuration. Interactions with advancement speed, not fully analysed in this study, could change partially the framework and should be further investigated.

References

- Anthony, D., Elbaum, S., Lorenz, A., Detweiler, C., 2014. On Crop Height Estimation with UAVs, IEEE/RSJ International Conference on Intelligent Robots and Systems, 4805-4012.
- Colomina, I., Molina, P., 2014. Unmanned aerial systems for photogrammetry and remote sensing: a review, ISPRS Journal of Photogrammetry and Remote Sensing, 92: 79-97.
- Costa, F. G., Ueyama, J., Braun, T., Pessin, G., Osorio, F. S., Vargas, P. A., 2012. The Use of Unmanned Aerial Vehicles and Wireless Sensor Network in Agriculture Applications, IEEE International Geoscience and Remote Sensing Symposium, .
- Hassan-Esfahani, L., Torres-Rua, A., Ticlavilca, A. M., Jensen, A., McKee, M., 2014. Topsoil Moisture Estimation for Precision Agriculture Using Unmanned Aerial Vehicle Multispectral Imagery, IEEE International Geoscience and Remote Sensing Symposium.
- MIT Technology Review, 2015. Agricultural Drones. Relatively cheap drones with advanced sensors and imaging capabilities are giving farmers new ways to increase yields and reduce crop damage, <http://www.technologyreview.com/featuredstory/526491/agricultural-drones/>.
- Primicerio, J., Di Gennaro, S. F., Fiorillo, E., Genesio, L., Lugato, E., Matese, A. , Vaccari, F. P., 2012. A flexible unmanned aerial vehicle for precision agriculture, Precision Agriculture, 13, 4: 517–523.
- Zhang, C., Kovacs, J. M., 2012, The application of small unmanned aerial systems for precision agriculture: a review, Precision Agriculture, 13,6:693–712